Inshore Migration of Japanese Eel *Anguilla japonica* Encouraged by Active Horizontal Swimming during the Glass Eel Stage

Tatsuro Karaki[1], Kei Sakamoto[2], Goro Yamanaka[2], Shingo Kimura[3], Akihide Kasai[4]
[1]Faculty of Life and Environmental Sciences, University of Tsukuba, Tsukuba, Japan
[2]Department of Atmosphere, Ocean, and Earth System Modeling Research, Meteorological Research Institute, Tsukuba, Japan
[3]Graduate School of Frontier Science, Atmosphere and Ocean Research Institute, The University of Tokyo, Kashiwa, Japan
[4]Faculty of Fisheries Sciences, Hokkaido University, Hakodate, Japan

*** Correspondence:**
Tatsuro Karaki
karaki.tatsuro.gm@u.tsukuba.ac.jp

Keywords: Japanese eel, glass eel, recruitment migration, numerical simulation, environmental DNA, diel vertical migration, horizontal swimming.

Abstract

The biomass of the Japanese eel (*Anguilla japonica*) is generally determined by the recruitment of glass eels into freshwater habitats, but the behavioral biology of their inshore migration remains unknown. With the aid of an ocean prediction system, we elucidated a recruitment migration scenario that can quantitatively reproduce a regional difference in biomass in Japan, which was previously estimated by an environmental DNA sampling method. For their successful reaching shores, it is necessary to incorporate behavioral changes of glass eels within their migration on the Kuroshio Current, such as shallower depth preferences and horizontal swimming towards lower salinity water. In particular, the latter is essential for encouraging recruitment into both the Seto Inland Sea with a relatively high ratio (20–30%) of the total recruitment to Japan and the coasts in the central part of the Pacific side of northern Japan (i.e., the northern limit of the habitable distribution), manifesting that glass eels actively swim towards freshwater near coastal regions. In the subsurface layer, where glass eels mainly conduct diel vertical migration, there is a bifurcation path connecting the Kuroshio current to the second and third branches of the Tsushima Warm Current, restricting recruitment of glass eels into the Sea of Japan side of the main inland in Japan. The simulated recruitment validated that the eDNA acts as a proxy indicator for estimating the relative biomass in the regional scale. The simulation supported that the inshore migration of glass eels is determined by active horizontal swimming.

Introduction

Catadromous fish breed in the sea but spend the majority of their adult lives in freshwater (Lalli and Parsons, 1997). Biomass is generally controlled by its recruitment to freshwater habitats during the pelagic larval stage. In general, larval dispersion from the spawning area to the nurseries is a major topic of fisheries management (Kasai et al., 1992; 2008), the details of which vary with species and remain mysterious. Since larvae have limited swimming ability, they are passively transported by oceanic currents at various temporal- and spatial-scales. However, they become active swimmers towards their preferred habitats after metamorphosing into juveniles. The dispersal patterns are essentially three-dimensional because of diel vertical migration (DVM), making larval sampling

difficult in the open ocean. Therefore, physical-biological numerical modeling approaches, in which the ocean general circulation model is coupled with a behavioral model of larvae and juveniles, are expected to reveal the role of each component and present a more plausible scenario for the recruitment process. In this study, attempts were made to address the return migration of the Japanese eel (*Anguilla japonica*) to the Japanese archipelago.

The Japanese eel is a catadromous fish that requires careful fishing management. Despite being designated as an endangered species, the Japanese eel is a commercially important fishery species in China, Taiwan, Korea, and Japan (Jacoby and Gollock, 2014). After the growth of Japanese eels in freshwater habitats of the eastern Asian-Pacific countries, mature adults conduct spawning migration for thousands of kilometers towards the southern part of the West Mariana Ridge, where the salinity front is established due to the Intertropical Convergence Zone (Tsukamoto, 1992, 2009; Kimura et al., 1994, 2001, 2006). Spawning of the Japanese eel likely occurs during the summer, with a peak between June and August (Ishikawa et al., 2001; Chow et al., 2009; Kurogi et al., 2011; Tsukamoto et al., 2011). Hatching and growth into larval fish (leptocephali) occur over several days (Tsukamoto, 2006). The leptocephali drift westward and northward by the North Equatorial and Kuroshio Currents, respectively and sequentially, although those entrained into the Mindanao Current flow towards the equator lapse into abortive migration (Kimura et al., 2006; Kim et al., 2007; Zenimoto et al., 2009). Metamorphosis into juvenile fish (glass eels) occurs near Taiwan (Shinoda et al., 2011; Fukuda et al., 2018), where glass eels generally arrive from November to February, with a sharp peak between December and January (Hsiung et al., 2022). The fishing season for glass eels in Japan is from December to April. The catch of wild glass eels has generally declined since the late 1970s (Kishida and Kanto, 2013; Kanto, 2015), indicating a decreasing trend in their recruitment. However, the specific cause is still unclear.

Previous numerical studies applied a ~10 km resolution ocean model to the larval transport of the Japanese eel and investigated how larval dispersal pathways can respond to synoptic-scale ocean-atmospheric changes. For example, virtual eels (v-eels) are more prone to entrainment into the Mindanao Current during El Niño events, in which a northward shift of the bifurcation latitude and a southward shift of the salinity front (i.e., spawning sea) simultaneously occur (Kim et al., 2007; Zenimoto et al., 2009; Lin et al., 2017; Hsiung et al., 2018). According to a forecast experiment (Hsiung and Kimura, 2019), abortive migration is more likely to occur due to global warming because it increases the frequency of El Niño events. Except for extreme El Niño events (e.g. 1997–98), realistically, they are not considerably correlated with the glass eel catches in Taiwan (Han et al., 2009). However, other climatic modes, such as the Quasi Biennial and Pacific Decadal Oscillations, do affect catches of glass eel in Taiwan (Tzeng et al., 2012). Recently, larval dispersal at low latitudes has been discussed from the viewpoint of a newly developed climate index known as the Philippines-Taiwan Oscillation (Chang et al., 2015, 2018a; Hsu et al., 2017).

Compared with the extensive knowledge of larval behaviors of glass eels in low latitudinal regions, the understanding of those in mid latitudinal regions, especially how they arrive in the freshwater habitats in East Asia, is limited due to the challenges in the study of glass eel migration. For example, glass eels gradually experience not only synoptic-scale circulations, such as the Kuroshio Current, mesoscale eddies, and shelf-break jets, but also smaller-scale phenomena, such as river plumes, bay circulations, and estuarine circulations. Numerically, dealing with these phenomena altogether requires a prohibitive running cost of the model with both a basin-scale domain and a fine horizontal resolution of less than 10 km. Observationally, the continuous monitoring of various rivers in East Asia seems impracticable because of the large survey areas and significant sampling efforts, although it is desirable to grasp an overall picture of glass eel recruitment.

Kasai et al. (2021), referred to as K21 hereafter, attempted to resolve these observational and numerical difficulties. K21 started with difficulties in monitoring the biomass of the Japanese eel. With the aid of the environmental DNA (eDNA) sampling method, K21 investigated the distribution of Japanese eels in rivers throughout Japan in a short period and found extremely low concentrations of their eDNA in Hokkaido (HK), the Sea of Japan side of northern Japan (JN), and northern part of the Pacific side of northern Japan (PN). The northern limit of eDNA detection (Fig. 1), though simply obtained by snapshot detections, was consistent with the natural distribution of Japanese eels as estimated using otolith stable isotope analyses and document investigations (Yoneta et al., 2019). In addition, the released number of farmed eels did not possess the same northern limit as the eDNA detection (see, Fig. 6 in K21). Although the eDNA concentration has still been an uncertain indicator of the biomass, it would be a good indicator for estimating the relative biomass, such as the regional difference in the abundance of the Japanese eel.

For validating the inferred biomass of the Japanese eel based on the eDNA surveys, K21 tried to simulate the recruitment number of glass eels into the Japanese rivers with the aid of the newest 2 km resolution ocean forecast system of the Japan Meteorological Agency (JMA), referred to as the JPN system (see the outlines in section 2). Here, the depth selected for v-eel migration was an important factor. For example, the arrival of glass eels in inland water areas requires their passage through shallow water areas above the coastal slope. Therefore, a well-known DVM model (e.g., Kim et al., 2007; Chang et al., 2018a; Hsiung and Kimura, 2019), based on the biology of leptocephali around the spawning area (Otake et al., 1998), cannot be applied to the inshore migration of glass eels as it is established that v-eels flow at a depth of ~150 m during the day and 50 m at night (i.e., in the subsurface layer). Instead, K21 regularly employed a shallower DVM within the surface layer to enable v-eels to come ashore, and showed that recruitment of v-eels released from the east of Taiwan to the northern limits is also limited.

However, the particle-tracking period of K21, corresponding with the fishing season for glass eels in Japan, was actually artificial and unnatural. As shown later in this study, in a longer tracking period, a regular application of the shallower DVM causes unrealistically high recruitment of v-eels into the Sea of Japan side of the main island of Japan. Hence, we hypothesized that glass eels exhibit a shift to a shallower layer in order to overcome the coastal slope, but behavioral change is limited near the coast. Furthermore, although the Seto Inland Sea (SI) yielded the highest detection rate of eDNA concentration among the respective composition ratios (~30% in Fig. 1b), v-eels without any horizontal swimming ability hardly entered there (see Fig. 4 in K21). Additionally, the particle-tracking simulation of K21 did not reproduce a higher eDNA concentration on the coast of PN (~14% in Fig. 1b). A common feature between the SI and PN coasts is that they are not directly along the path of the Kuroshio Current, and therefore, passive transport by ocean currents may be insufficient to recruit glass eels into such frontier habitats.

We hypothesized that active horizontal swimming plays an essential role in promoting inshore migrations. Yamada et al. (2009) conducted a laboratory study and reported that glass eels can swim at an average speed of ~5 cm s^{-1}. However, the factors governing swimming direction remain unclear. Therefore, previous numerical studies considered several swimming scenarios: parallel swimming along background flow (Chang et al., 2015); fixed directional swimming towards the coast (Chang et al., 2018b); and flexible directional swimming towards lower salinity water (Hsiung and Kimura, 2019). The first scenario does not permit v-eels to swim against ocean currents, such as the outflow from the Seto Inland Sea. The application of the second scenario to the Japanese archipelago is not easy because of the complicated coastal topographies that are surrounded by different seas from all directions. For simplicity, we here adopted the last scenario based on the fact that the preference for lower-salinity

water of glass eels has been demonstrated through laboratory studies (Tosi et al., 1990; Fukuda et al., 2019; Kumai et al., 2021).

Thus, numerical modelling approaches have not validated the spatial variations in biomass of the Japanese eel estimated by the eDNA surveys (Fig. 1) yet. Therefore, this study revisited the particle-tracking simulation of K21, using a more plausible scenario on the migration biology of glass eels. The JPN system, which contains data on a detailed coastal topography around Japan and diluted water due to river runoff and resultant coastal salinity fields (Sakamoto et al., 2019), was found suitable for the examination of our hypotheses about eels' shallower depth preference and active horizontal swimming towards lower salinity to reach shores. We first demonstrated the sensitivity of the passive transport of v-eels to water depth by applying different DVM scenarios. We then showed that a horizontal swimming model based on a preference for lower salinity water resulted in more quantitative reproducibility of regional differences in the eDNA detection rate of Japanese eels (Fig. 1).

Materials and methods

The recruitment migration of Japanese eels was simulated using the output data of the JPN system (Formal name: MOVE/MRI.COM-JPN system) (see Sakamoto et al. (2019) and Hirose et al. (2019) for a more detailed explanation of the JPN system). The simulation results were validated using eDNA sampling data from Japanese eels (Fig. 1; see K21 for more detailed information). The core of the JPN system was a ~2 km horizontal resolution model with an analytical domain spanning from 117–160 E and 20–52 N, covering the coastal seas around Japan. The core model was coupled to the parent models, whose domains were global and North Pacific, respectively, by double two-way nesting, so that the JPN system describes oceanic variations in coastal regions matching the basin scale. The JPN system was also assimilated into observational data concerning *in-situ* temperature and salinity, satellite sea surface temperature and height, and sea ice concentration based on a data assimilation method called incremental 4D-VAR. As a result, the JPN system provided a more reliable forecast of the behavior of mesoscale and fine-scale oceanic phenomena (e.g., coastal fronts and low-salinity river plumes) based on the realistic evolution of synoptic-scale phenomena (e.g., the Kuroshio Current and mesoscale eddies). The coastal topography around Japan, whose minimum depth is set to 8 m in the JPN system, was also well reproduced by the depth coordinates at 60 vertical levels with variable vertical resolutions from 2 m at the sea surface to 700 m at the sea floor. At the sea surface, 5 km of resolved wind and pressure forcing of the Meso-Scale Model reanalysis (JMA) and 55 km of resolved radiation, precipitation, temperature, and dew point temperature of JRA55do (Tsujino et al., 2018) were enforced at 1 and 3 h intervals, respectively. The introduction of the eight main tidal constituents (M2, S2, N2, K2, O1, K1, P1, and Q1 (Sakamoto et al., 2013)) and ~4,000 river inflows across Japan enable the JPN system to reproduce basic fields and short-term variations in coastal regions, especially in coastal areas such as the Seto Inland Sea (Sakamoto et al., 2019).

We analyzed the output data of the JPN system spanning 2008–2017 based on the assumption that glass eel recruitment during this period would cause regional differences in the eDNA detection rate of Japanese eels (Fig. 1). Similar to K21, larval pathways in this study were simulated from the daily averaged horizontal velocity field while applying linear interpolation in time and space. Therefore, tidal currents and resultant diffusions were not included explicitly in our particle-tracking simulations, although the influences on larval dispersal are discussed later. V-eels move based on the evolution equation $D\boldsymbol{x}/Dt = \boldsymbol{u} + \boldsymbol{u}^*$, where $\boldsymbol{x}$ is the two-dimensional trajectory of a v-eel, $\boldsymbol{u}$ represents the horizontal oceanic flow field, and $\boldsymbol{u}^*$ represents the horizontal swimming of a v-eel as estimated by the surface salinity field. This equation was resolved using the fixed-step 4th-order Runge-Kutta

integration method. We tested the performances at different time intervals and found that 3 h was an appropriate choice in terms of sensitivity to v-eel pathways and numerical cost.

Our discussion first excluded horizontal swimming, $\boldsymbol{u}^*$, to examine whether passive transport of v-eels by ocean currents can quantitatively reproduce the habitable distribution of Japanese eels (Fig. 1). We employed two DVM scenarios, although concerning the DVM in shallower regions (e.g., the Yellow Sea with a maximum depth of ~150 m), an adjustment in which v-eels are transported by bottom currents was applied to all scenarios to prevent their subduction under the seafloor. In the first scenario (referred to as the CTRL scenario), v-eels flow at a depth of 150 m during the day (6 a.m.–6 p.m.) and 50 m at night (6 p.m.–6 a.m.). Hence, v-eels in the CTRL scenario follow the conventional DVM model in the open ocean, whereas the inshore migration above the coastal slope occurs within the bottom boundary layer owing to the adjustment mentioned above. Second (referred to as the SURF scenario), a shallower DVM was imposed between depths of 50 m and 1 m. The purpose of the SURF scenario was to examine the possibility that glass eels were consistently within the surface layer during recruitment migration. Therefore, the SURF scenario was identical to the particle-tracking simulation of K21 in terms of the regular application of the shallower DVM. Although we conducted additional experiments with different reference depths (not shown), the results were similar to those of the CTRL and SURF scenarios. Consistently, a previous study has reported that v-eel migration is not sensitive to small changes in depth (Chang et al., 2016).

The third (COMB) and fourth (SWIM) scenarios emphasize the importance of behavioral changes in glass eels in addition to passive transport by ocean currents. In the COMB scenario, the DVM model was the same as that in the CTRL scenario in the open ocean but changed in the SURF scenario, where v-eels were within ~10 km of the coast (referred to as the near-coastal region). Unlike in the SURF scenario, in the COMB scenario, the application of the shallower DVM was limited near the coast. Therefore, the COMB scenario was used to evaluate a hypothesis concerning the inshore migration that glass eels exhibit shallower depth preference near the coast, thereby overcoming the coastal slope. In the SWIM scenario, the DVM model was the same as in the COMB scenario; however, active horizontal swimming was introduced only in the near-coastal region during the night, and v-eels swimmed along the sea surface. The SWIM scenario revealed the influence of active horizontal swimming on the inshore migration of glass eels. Each v-eel in the SWIM scenario could swim at a speed of 5 cm s^{-1} from the current position towards the lowest salinity point in the cardinal and intermediate directions (i.e., N, S, E, W, NE, SE, NW, and SW points). The determination of swimming direction was based on the daily average sea surface salinity field of the JPN system. In the JPN system, salinity grid points were not superimposed on the velocity points based on the Arakawa B-grid. Therefore, we calculated salinity at the velocity grid points by a 4-point area average. The minimum spatial resolution of the simulated eddy is generally 5–10 times the grid size (Levy et al., 2012). For v-eels to easily transfer to a neighboring eddy, we assumed that they could recognize the surrounding salinity beyond five grids (~10 km).

Initially, there were ~300,000 particles set to the east of Taiwan (black parallelogram in Fig. 2) with a spatial interval of 0.0025°. For the generality of the results, the tracking period after release was one year, which was approximately three times as long as that of the particle-tracking experiment of K21. The recruitment success of v-eels at each coastal point was estimated using the cumulative number of v-eels approaching the shore within a radius of ~2 km. The regional composition of the total recruitment number, divided into eight coasts (HK, PN, PE, PW, SI, KS, JW, and JN coasts; Fig. 1), was used for a direct comparison with those from eDNA detection (Fig. 1). Considering the arrival period of glass eels off Taiwan (Hsiung et al., 2022), we conducted ensemble experiments every year

during 2008–2017, where the release dates were November 15, December 1 and 15, January 1 and 15, and February 1 of every year, and discussed the composite results.

Results

We outlined the simulation results for each scenario based on the visitation frequency of v-eels in coastal seas around Japan (Fig. 3) and within the SI coast (Fig. 4), the recruitment success number at each coastal point (Fig. 5), and the regional compositional ratio of the total amount (Fig. 6), all of which are decadal mean descriptions.

a. CTRL scenario: larval passive transport at 50–150 m depths

The major paths of v-eel recruitment migration in the CTRL scenario are described as regions with a higher visitation frequency (the red part in Fig. 3a). Most v-eels are transported northeastward by the Kuroshio Current from east of Taiwan and bifurcated into eastward and northward directions around 127° E and 30° N. The eastward bifurcation path accomplishes a relatively high recruitment success along the KS, PW, and PE coasts (red points in Fig. 5a) because v-eels continue to float on the Kuroshio Current. However, the number of v-eels reaching the PN coast and northward that are not along the path of the Kuroshio Current is approximately two orders of magnitude fewer (black points in Fig. 5a). In the northward bifurcation path, v-eels were entrained into the second and third branches of the Tsushima Warm Current after floating via Cheju Island and the western channel of the Tsushima Strait (Fig. 3a), thereby restricting recruitment success to the JW and JN coasts. Although v-eels can disperse to the HK coast far from the main paths, their recruitment success is relatively low. The recruitment distribution of the CTRL scenario (Fig. 5a) exhibited a similar northern limit for eDNA detection in Japanese eels (Fig. 1). More quantitatively (Fig. 6), minor composition ratios in the HK, JN, and JW coasts of eDNA concentration (black) were well reproduced by recruitment migration in the CTRL scenario (gray).

However, the CTRL scenario does not account for the migration biology of glass eels when it comes to their recruitment into the SI coast. The visitation frequency (Fig. 4a) of the SI coast is almost zero in the interior because v-eels in the CTRL scenario cannot pass through the Bungo and Kii channels. Recruitment success results in only ~5% of the total amount (Fig. 6), which is insufficient compared to the high eDNA concentration on the SI coast (~30%). In addition, the recruitment of v-eels into the PN coast was restricted to the southern part (Fig. 3a and 5a), resulting in a lower recruitment success rate (~5%) than that of the eDNA concentration (~14%). On the other hand, the CTRL scenario led to an excessive recruitment success of over 50% on the KS coast, although the eDNA concentration was ~20% (Fig. 6).

b. SURF scenario: larval passive transport at 1–50 m depths

The SURF scenario enables v-eels to penetrate the Bungo channel (Fig. 4b), resulting in their successful recruitment in the interior of the SI coast (Fig. 5b). The eastward dispersal of v-eels in the interior of the SI coast reflects the simulated throughflow passage from the Bungo to the Kii channels in the JPN system, which was consistent with previous numerical studies (e.g., Yoshinari et al., 2020). However, as shown by the green bars in Fig. 6, the composition ratio of the SI coast is still extremely low (~5%), as those of the JW and JN coasts dramatically increase by over 30%. In the SURF scenario, most v-eels that bifurcate from the Kuroshio Current pass through the eastern channel of the Tsushima Strait and board the first branch of the TWC (Fig. 3b), providing a clockwise migration passage along JW and JN along the northern part of the PN coast via the Tsugaru Strait. As a result, the geographical

distribution of recruitment success (Fig. 5b) does not satisfy the northern limits of the habitable distribution of Japanese eels (Fig. 1a).

c. COMB scenario: same as the CTRL scenario, but for varying to the SURF scenario in the near-coastal region

In the COMB scenario, the limitation of arrival at the HK, JN, and JW coasts and the penetration of v-eels into the SI coast through the Bungo Channel are reproduced altogether (Figs. 3c, 4c, and 5c). This improvement in reproducibility is a result of the limited application of the shallower DVM only in the near-coastal region, implying that the migration biology of glass eels can be divided into pelagic and coastal stages. However, for promoting the shoreward migration, the daily mean surface current in the near coastal region seems insufficient because of the lower recruitment success on the SI coast (~10%: blue bars in Fig. 6). In addition, due to the lack of v-eel recruitment into the PN coast (Fig. 5c), the recruitment success at the PN coast becomes less than 3% (Fig. 6), widening the gap to the eDNA concentration (~14%) compared with that of the CTRL and SURF scenarios.

d. SWIM scenario: same as COMB scenario, but for permitting active horizontal swimming

In the SWIM scenario, the visitation frequency in near-coastal regions generally increased by one order of magnitude compared to the COMB scenario (Fig. 3c and 3d). Remarkably, active horizontal swimming dramatically improved the penetration of v-eels into the SI coast (Fig. 4c and 4d). In particular, the inflow of v-eels occurs not only through the Bungo Channel but also through the Kii Channel, in which the simulated outflow from the SI coast to the Pacific Ocean is present. The comparison in recruitment success (Fig. 5c and 5d) also emphasizes the intensification of v-eel penetration into the bay areas on the Pacific side. In addition, many v-eels could move northward along the PN coast up to the middle point (Fig. 3d and 5d). Compared with these main habitats, the recruitment success to the JE and JN coasts seems to be one order of magnitude lower (Fig. 5d), whereas those to the HK coast and the northern part of the JN coast are further limited. As a result, the spatial distribution of the recruitment amount in the SWIM scenario (Fig. 5d) can consistently explain the eDNA detection in Japanese eels (Fig. 1a), including the northern limit on the Pacific side, both of which were consistent with the natural distribution (Yoneta et al., 2019). More quantitatively (red bars in Fig.6), the SI coast (~20%) is one of the major nursery habits, and the PE (~25%), PW (~15%), and KS (~25%) coasts, but the HK (~1%), JW (~5%), and JN (~1%) coasts do not. In terms of reproducing the eDNA concentration (~14%), the SWIM scenario (~8%) is the most plausible among the three scenarios for recruitment success at the PN coast.

Discussion

a. The best scenario in this study

The SWIM scenario led to the highest quantitative reproducibility in the regional composition ratios of eDNA concentration in Japanese eels, indicating that active horizontal swimming is essential for the inshore migration of glass eels. Three other scenarios result in apparent inconsistencies: v-eels in the CTRL scenario hardly entered the SI coast, which is one of the major nursery habits, whereas those in the SURF scenario unrealistically exceeded the northern limits of the habitable distribution. Although the COMB scenario that can reproduce both northern limits on the Sea of Japan side and recruitment migration into the SI coast was the best scenario among the passive larval transport simulations in this study, it performed worse in terms of reproducibility in the northern limit on the Pacific side.

Major defects in the CTRL scenario indicate that the assumption that v-eels float along the seafloor (i.e., via the bottom boundary layer) when approaching a shore would be problematic. From a physical oceanographic point of view, the inshore bottom Ekman transport beneath the Kuroshio Current produces high recruitment success in the southeastern part of the KS coast (Fig. 5a). Although such Ekman transport effectively carries v-eels along the PN coast, the carriage is only up to the southern part and does not approach the northern limit. In the JPN system, the outflows from the SI coast mainly occur above the seafloor, as shown in previous studies (e.g., Uchiyama et al., 2012), obstructing the penetration of v-eels from the open ocean through the Bungo and Kii channels.

Consistent with the interpretations mentioned above, the inshore migration of v-eels in the SURF scenario shows different behavior from that in the CTRL scenario. For example, recruitment into the SI coast increased, whereas recruitment into the southeastern part of the KS coast and the southern part of the PN coast decreased (Fig. 5b). However, if the SURF scenario is correct, the Sea of Japan side of the main inland area in Japan has become the most commercial fishing ground, which is empirically wrong. Therefore, the recruitment migration of glass eels does not seem to follow the SURF scenario (i.e., regular application of a shallower DVM than at a depth of ~50 m). This implies that the vertical migration of glass eels into the surface layer may be minor in the open ocean. The particle-tracking simulation of K21, in which a similar shallow DVM was applied, will reach the same conclusion as our SURF scenario if their tracking period extends several months from the end of April.

A comparison between the CTRL and SURF scenarios (Fig. 3a and 3b) also clarifies how the Kuroshio Current bifurcates in the East China Sea. The bifurcation current in the CTRL scenario (i.e., through subsurface or bottom layers) flows along ~100 m isobath (the boundary between the blue and green colored shades in Fig. 2) and then circulates around the Korean Peninsula while seeing the left-hand side of the coast, whereas that in the SURF scenario (i.e., through the surface layer) flows around the main island of Japan to the right-hand side. The adjustment process by topographic waves seems to play an essential role in setting the bifurcation currents; the former is established by shelf waves propagating southwestward along ~100 m isobath (Liu et al., 2021); the latter is done by coastally trapped waves propagating cyclonically around the main island of Japan that are excited at the Pacific side (Tsujino et al., 2008; Kida et al., 2016). Previous tracer experiments (Guo et al., 2006) also reported a similar sensitivity of bifurcation paths to depth.

The COMB scenario (i.e., shallower depth preference in the near-coastal region) does not quantitatively explain the behavioral change of glass eels when they reach coastal nursery habitats (Fig. 6). Although this result suggests that passive transport through ocean currents is not the only factor that can control the recruitment migration of glass eels, our particle-tracking simulations do not explicitly include tides. Tidal currents and resultant horizontal mixing play a key role in exchanges between pelagic and coastal waters. This process could be another important environmental factor responsible for the onshore migration of glass eels. The JPN system includes tides; however, because of our limited numerical resources, we used the daily mean velocity fields in which tidal currents are nearly excluded except for residual currents. Instead, we showed a possible strategy for glass eels to reach the shore by introducing active horizontal swimming. Fukuda et al. (2016) observed an enhancement of glass eel recruitment during the flood tide in the new moon. Therefore, we hope that future work with plentiful numerical resources can numerically investigate the relationship between tides and glass eel recruitment, and that particle-tracking experiments, especially following the COMB scenario, may be useful as sensitivity experiments without tides.

b. Comparison with previous studies

Previous numerical studies (Rypina et al., 2014; Chang et al., 2018b) considered that the active horizontal swimming of glass eels would play a leading role in their escape from wind-driven circulation. On the other hand, in the SWIM scenario, v-eels can diffusively leave the Kuroshio Current first, despite excluding any diffusion terms (i.e., random walk) from the particle tracking scheme, and then swim towards freshwater habitats. This result is approximately unchanged if active horizontal swimming is imposed from the release, because their swimming speed (5 cm s^{-1}) is much slower than the Kuroshio Current (> 100 cm s^{-1}) and associated mesoscale eddies (10–40 cm s^{-1}) in the open ocean (not shown). Thus, we consider that the horizontal swimming of glass eels would be an active adjustment to the recruitment distribution that could be passively determined by ocean currents beforehand. As a result, they can arrive at frontier habitats such as the SI and PN coasts.

In this study, the influence of salinity on the habitat selection of glass eels collected by laboratory studies (e.g., Tosi et al., 1990) was quantitatively evaluated in a more realistic situation. However, it has been unknown how far glass eels can detect the surrounding salinity in the ocean. The detection range depended on the horizontal grid of the JPN system and did not reflect the actual distance. Instead, we quantitatively clarified that whether glass eel recruitment is determined by ocean currents passively or horizontal swimming actively is an essential question in the inshore movement. Although the importance of the latter may be underlined by the SWIM scenario, it contained only part of the biology of glass eels. For example, neither the preference for water with a rich river-originated odor (Fukuda et al., 2019) nor locomotor activities promoted by higher water temperature (Kumai et al., 2021) were included. The assessment of several biological models will make it easier to focus on the migration of glass eels from a near-coastal region to an estuary using a realistic estuary model with a finer horizontal resolution than the JPN system.

It is noteworthy that v-eels were zonally and meridionally well diffused in all scenarios (Fig. 3) compared with previous numerical results (e.g., Zenimoto et al., 2009; Chang et al., 2015; Hsiung et al., 2018). This gap arises from the difference in the horizontal resolution of the ocean model and the resultant reproducibility in mesoscale eddies with a diameter of 10 km. Recently, Chang et al. (2017) argued the eddy trapping ability of v-eels using a ~10 km resolution ocean model and reported a negative relationship between glass eel catches in Taiwan and the abundance of eddies in the eastern sea, called the Subtropical Counter Current eddy zone. The application of a higher resolution model, such as the JPN system, may further support their arguments because the horizontal eddy diffusion is possibly intensified during the eddy-rich year, thereby preventing v-eels from going on board the Kuroshio Current.

Successful fishery management of Japanese eels should be established based on a reasonable prediction algorithm for glass eel catches and the high season of their arrival. As shown by Aoyama et al. (2016), a delayed peak in their arrival in several months occasionally obstructs the decision on the proper fishing season, possibly resulting in a poor catch of glass eels. Here, we briefly discuss possible causes. The best scenario in this study (i.e., the SWIM scenario) predicts that the arrival of glass eels in the main nursery habitats (i.e., the KS, JW, and JE coasts) will occur within ~1–2 months after they pass the eastern part of Taiwan (Fig. 7a), and that inter-annual variability in their arrival date would be within ~5–10 days (Fig. 7b). In terms of the arrival date, the recruitment migration of glass eels from Taiwan may inherently not possess major temporal variability. Therefore, it is reasonable that the fishing season of glass eels be regulated from December to April if their arrival in Taiwan ordinarily occurs from November to February. One drawback of our larval transport simulations is that the release of v-eels is temporally and quantitatively constant, although glass eel catches in Taiwan have exhibited multi-timescale variability (Tzeng et al., 2012). As a result, inter-annual variations in glass eel catches

in Japan, such as the year of the poor catch in 2013 (Fisheries Agency of Japan), were not reproduced in our numerical simulations (not shown). To reproduce these results, future numerical research should reflect inter-annual variations in glass eel catches in Taiwan as more realistic initial conditions.

c. Validation of eDNA information

According to Shelton et al. (2019), the eDNA information correlates highly with the biomass estimated by the seine survey on the population scale, although the correlation was reduced at the site scale. In this study, eight coasts (i.e., HK, PN, PE, PW, SI, KS, JW, and JN coasts in Fig. 1b) and individual rivers represent the population scale and the site scale, respectively. We estimated how the eDNA information reflects the true abundance from the viewpoint of the numerical modelling approach. As a result, it was found that at the population scale, the simulated recruitment numbers well reflect the spatial variations in the inferred biomass based on the eDNA surveys (Fig. 6). Therefore, as well as Shelton et al. (2019), we consider that the eDNA information possibly becomes a good indicator for estimating the relative biomass in the population scale. More concretely, a higher recruitment success of glass eels possibly produces a higher abundance of the Japanese eel, resulting in a higher eDNA concentration. Shelton et al. (2019) also indicated that the eDNA information may act to smooth otherwise patchy biological signals in space and time. This would be one possible reason that enables our direct comparison between the eDNA snapshot data and the decadal-mean simulation data.

Conclusions

The recruitment process and biological change of the glass-eel stage in Japanese eels are essentially unknown. In this study, we presented a more plausible recruitment scenario of glass eels that can reproduce the spatial variations in biomass of the Japanese eel estimated by the eDNA surveys. The main finding of this study is that the subsurface-layer flow of the Kuroshio Current seems to lay the groundwork for the recruitment migration of glass eels into Japan. So, the coastal regions that are not along the path of the Kuroshio Current, such as the HK coast and the northern part of the PN coast, appear not to become the nursery habitats, and neither do those on the Sea of Japan side (JW and JN coasts), as a matter of course. We further found an additional factor possibly preventing glass eels from reaching the latter: in the subsurface layer, there is a bifurcation path from the Kuroshio Current to the eastern part of the Korean Peninsula through the western channel of the Tsushima Strait, resulting in less entrainment of glass eels into the first branch of the Tsushima Warm Current that flows northeastward along the main island of Japan. That is, the habitable distribution of Japanese eels in Japan, especially the northern limit on the Sea of Japan side (Fig. 1), is a result of glass eels passively transported by ocean currents while conducting the DVM within the subsurface layer. Therefore, the conventional assumption that leptocephali and glass eels conduct similar DVMs is validated, but the applicability coverage is possible during the pelagic stage. In the coastal stage of glass eels, biological changes such as changing depth preference and active horizontal swimming would play an essential role in their inshore migrations. In particular, the swimming model reflecting the preference for lower salinity water dramatically encouraged the inshore migration of glass eels, thereby improving the reproducibility of recruitment into the interior of the SI coast (i.e., one of the major nursery habits) and the southern and central parts of the PN coast (i.e., the northern limit of the habitable distribution of Japanese eels on the Pacific side). Conclusively, the simulation supported that the inshore migration of glass eels is determined by active horizontal swimming.

Figures

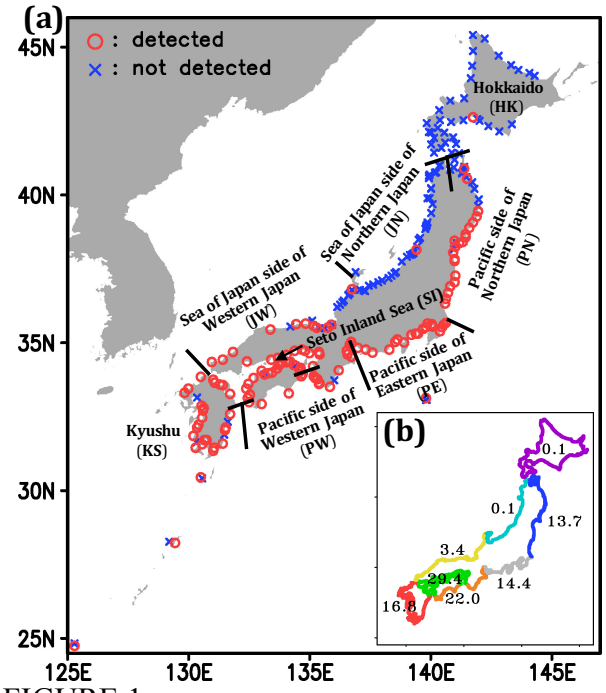

FIGURE 1

Map for detection of *Anguilla Japonica* eDNA in Japan (a); and the regional composition ratio to total eDNA concentration (b), from Kasai et al. (2021), though processed without loss of originality. HK, Hokkaido; PN, PE, and PW, Pacific side of northern, eastern, and western Japan, respectively; SI, Seto Inland Sea; KS, Kyushu; JW and JN, Sea of Japan side of western and northern Japan, respectively.

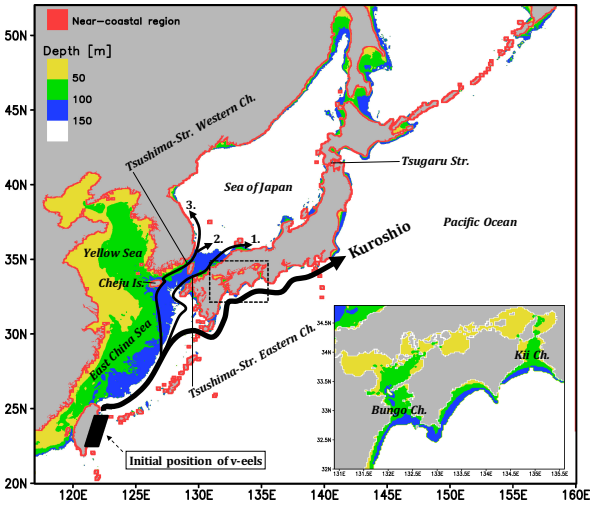

FIGURE 2

Model domain, bathymetry (yellow, green, blue, and white color shades), and geographical location of ocean currents (black thick arrows). Numbers 1, 2, and 3 indicate the first, second, and third branches of the Tsushima Warm Current, respectively. Near-coastal regions are exhibited by red color. The initial position of v-eels (black parallelogram) is located in the east of Taiwan.

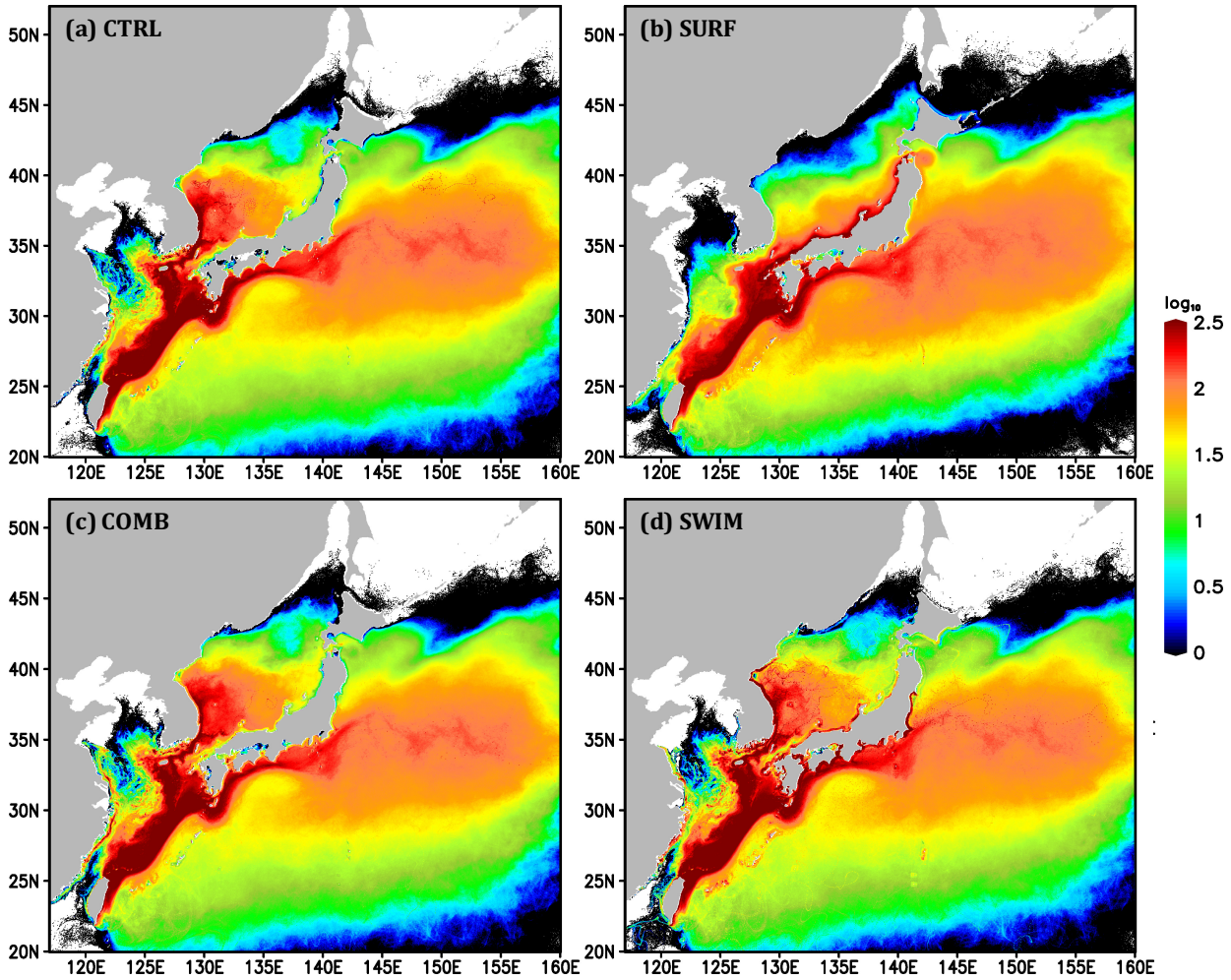

FIGURE 3

Decadal mean visitation frequency of v-eels in CTRL (a); SURF (b); COMB (c); and SWIM (d) scenarios, expressed on a log-scale.

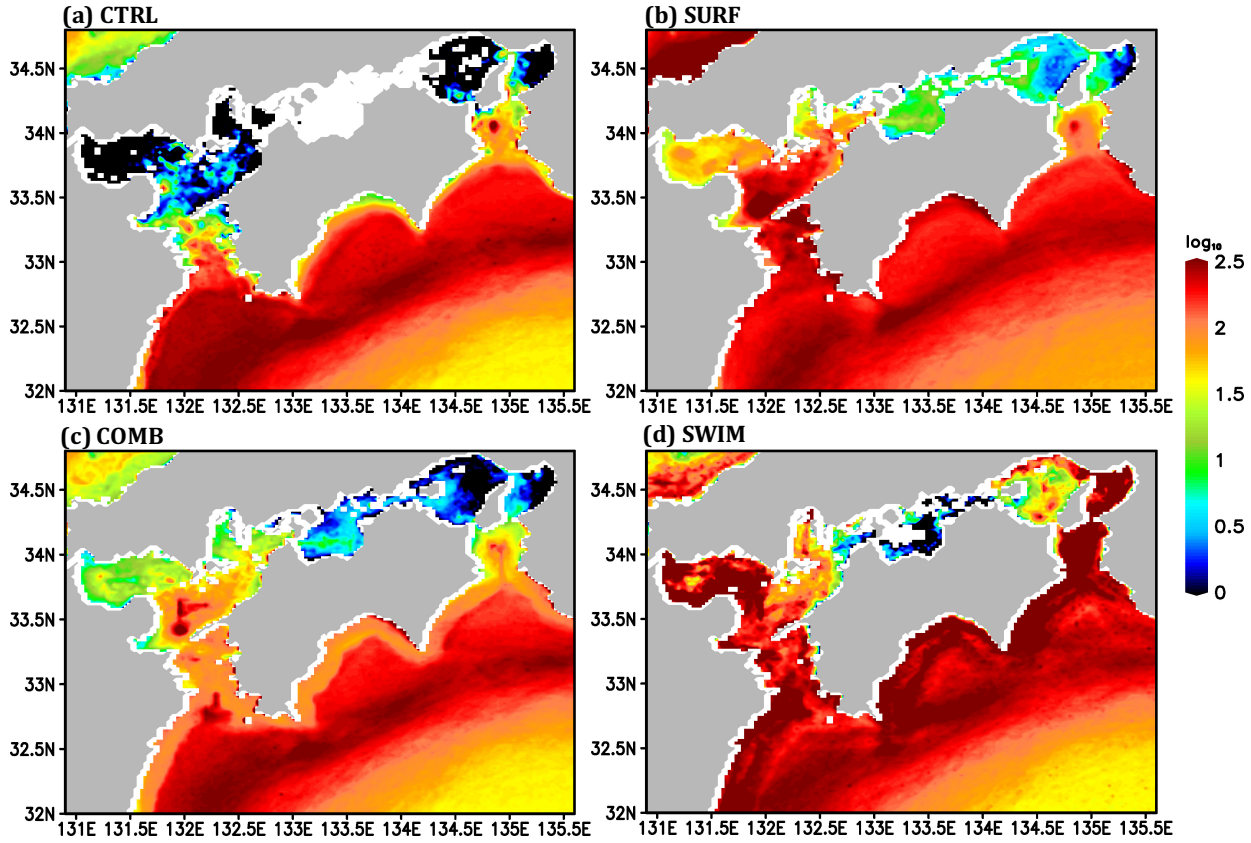

FIGURE 4
Decadal mean visitation frequency of v-eels at the Seto Inland Sea in CTRL (a); SURF (b); COMB (c); and SWIM (d) scenarios, expressed on a log-scale.

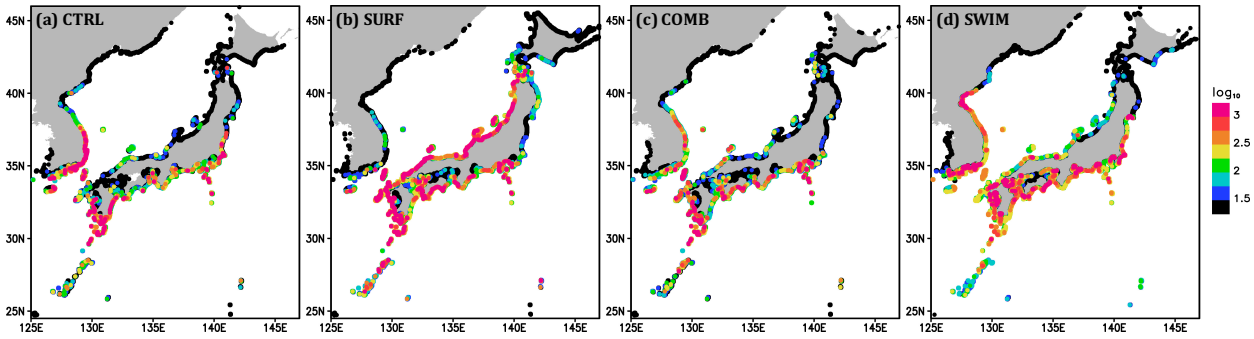

FIGURE 5
Decadal mean recruitment success number of v-eels at each coastal point in CTRL (a); SURF (b); COMB (c); and SWIM (d) scenarios, expressed in a log-scale.

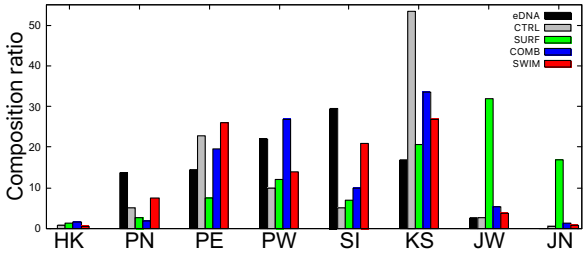

FIGURE 6
Direct comparisons of the regional composition ratio to total eDNA concentration (from Fig. 1b) and those of total recruitment success number of v-eels in respective scenarios (from Fig. 5). HK, Hokkaido; PN, PE, and PW, Pacific side of northern, eastern, and western Japan, respectively; SI, Seto Inland Sea; KS, Kyushu; JW and JN, Sea of Japan side of western and northern Japan, respectively.

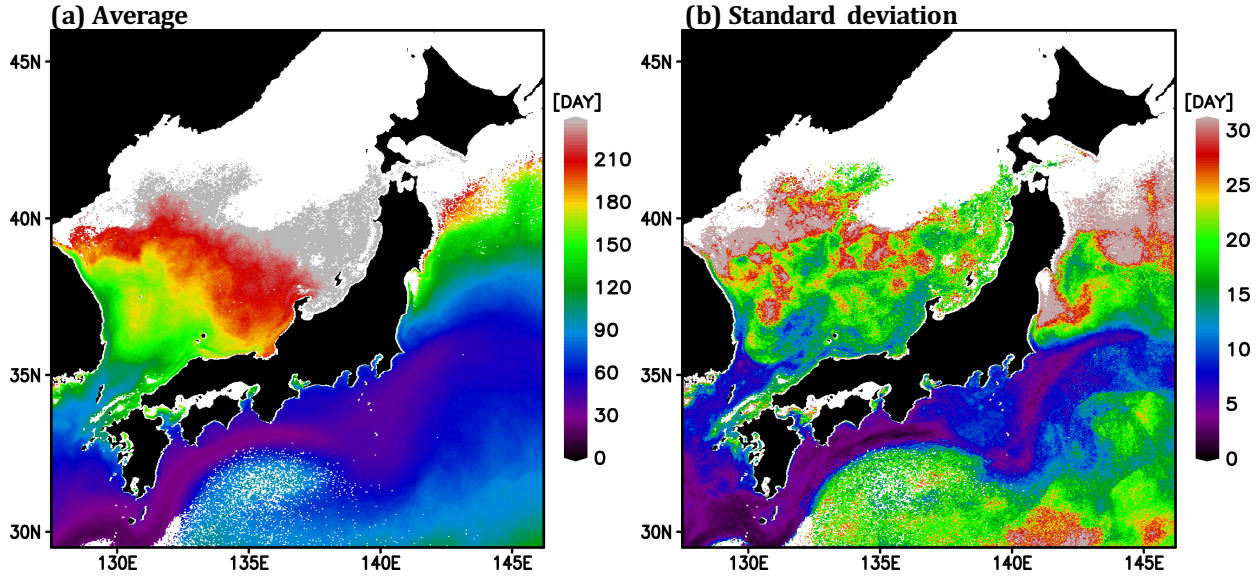

FIGURE 7
Decadal mean advection times of v-eels from the eastern part of Taiwan to respective grid points around Japan (a); and the standard deviation (b) in SWIM scenario. For simplicity, the calculations are done only at grid points where v-eels pass in the whole ensemble experiments.

Data Availability Statement

The original contributions presented in the study are included in the article/supplementary material, and further inquiries can be directed to the corresponding author.

Ethics Statement

Ethical review and approval were not required for the study as it did not treat any vertebrate directly.

Author Contributions

AK conceived and designed the experiment, and TK and KS conducted numerical simulations. TK wrote the manuscript. All authors discussed the results, contributed critically to the manuscript, and agreed to be accountable for the content of this work.

Funding

Part of this study was supported by JSPS KAKENHI, Grant-in-Aid for Scientific Research (A), Grant Number17H01412, and by the Cooperative Program (No. 102, 2021) of the Atmosphere and Ocean Research Institute, The University of Tokyo.

Acknowledgments

We would like to thank Editage (www.editage.com) for the English language editing and two anonymous reviewrs for their improvements of this manuscript.

References

Aoyama, J., Shinoda, A., Yoshinaga, T., and Tsukamoto, K. (2012). Late arrival of *Anguilla japonica* glass eels at the Sagami River estuary in two recent consecutive year classes: ecology and socio-economic impacts. *Fish. Sci.*, 78, 1195-1204. doi: 10.1007/s12562-012-0544-y

Chang, Y. L., Sheng, J., Ohashi, K., Béguer-Pon, M., and Miyazawa, Y. (2015). Impacts of interannual ocean circulation variability on Japanese eel larval migration in the western North Pacific Ocean. *PloS ONE*, 10(12), e0144423. doi: 10.1371/journal.pone.0144423

Chang, Y. L., Miyazawa, Y., and Béguer-Pon, M. (2016). Simulating the Oceanic Migration of Silver Japanese Eels. *PLoS ONE*, 11(3), e0150187. doi: 10.1371/journal.pone.0150187

Chang, Y. L., Miyazawa, Y., and Béguer-Pon, M. (2017). The dynamical impact of mesoscale eddies on migration of Japanese eel larvae. *PLoS ONE*, 12(3), e0172501. doi: 10.1371/journal.pone.0172501

Chang, YL. K., Miyazawa, Y., Miller, M. J., and Tsukamoto, K. (2018a). Potential impact of ocean circulation on the declining Japanese eel catches. *Sci. Rep.*, 8, 1-12. doi: 10.1038/s41598-018-23820-6

Chang, Y. L. K., Miller, M. J., Tsukamoto, K., and Miyazawa, Y. (2018b). Effect of larval swimming in the western North Pacific subtropical gyre on the recruitment success of the Japanese eel. *PloS ONE*, 13, e0208704. doi: 10.1371/journal.pone.0208704

Chow, S., Kurogi, H., Mochioka, N., Kaji, S., Okazaki, M., and Tsukamoto, K. (2009). Discovery of mature freshwater eels in the open ocean. *Fish. Sci.*, 75, 257-259. doi: 10.1007/s12562-008-0017-5

Fukuda, N., Kurogi, H., Ambe, D., Chow, S., Yamamoto, T., Yokouchi, K., Shinoda, A., Masuda, Y., Sekine, M., Saitoh, K., Masujima, M., Watanabe, T., Mochioka, N., and Kuwada, H. (2018). Location, size and age at onset of metamorphosis in the Japanese eel *Anguilla japonica*. *J. Fish Biol.*, 92, 1342-1358. doi: 10.1111/jfb.13590

Fukuda, N., Yokouchi, K., Yamamoto, T., Kurogi, H., and Yada, T. (2019). Salinity and odor preferences of Japanese el during the first year of post-recruitment growth in saline water. *J. Ethol.*, 37, 93-99. doi: 10.1007/s10164-018-0572-x

Guo, X., Miyazawa, Y., and Yamagata, T. (2006). The Kuroshio onshore intrusion along the shelf break of the East China Sea: The origin of the Tsushima Warm Current. *J. Phys. Oceanogr.*, 36, 2205-2231. doi: 10.1175/JPO2976.1

Han, Y. S., Tzeng, W. N., and Liao, I. C. (2009). Time series analysis of Taiwanese catch data of Japanese glass eels *Anguilla japonica*: possible effects of the reproductive cycle and El Niño events. *Zool. Stud.*, 48, 632-639.

Han, Y. S., Hsiung, K. M., Zhang, H., Chow, L. Y., Tzeng, W. N., Shinoda, A., Yoshinaga, T., Hur, S. P., Hwang, S. D., Iizuka, Y., and Kimura, S. (2019). Dispersal characteristics and pathways of Japanese glass eel in the East Asian continental shelf. *Sustainability*, 11(9), 2572. doi:10.3390/su11092572

Hirose, N., Usui, N., Sakamoto, K., Tsujino, H., Yamanaka, G., Nakano, H., Urakawa, S., Toyoda, T., Fujii, Y., and Kohno, N. (2019). Development of a new operational system for monitoring and forecasting coastal and open-ocean states around Japan. *Ocean Dyn.*, 69, 1333-1357. doi: 10.1007/s10236-019-01306-x

Hsiung, K. M., Kimura, S., Han, Y. S., Takeshige, A., and Iizuka, Y. (2018). Effect of ENSO events on larval and juvenile duration and transport of Japanese eel (*Anguilla japonica*). *PLoS ONE*, 13, e0195544. doi: 10.1371/journal.pone.0195544

Hsiung, K. M. and Kimura, S. (2019). Impacts of global warming on larval and juvenile transport of Japanese eels (*Anguilla japonica*). *Deep Sea Res. Part II: Topical Studies in Oceanography*, 169, 104685. doi: 10.1016/j.dsr2.2019.104685

Hsiung, K. M., Lin, Y. T., and Han, Y. S. (2022). Current Dependent Dispersal Characteristics of Japanese Glass Eel around Taiwan. *J. Mar. Sci. Eng.,* 10, 98. doi: 10.3390/jmse10010098

Hsu, A. C., Xue, H., Chai, F., Xiu, P., and Han, Y. S. (2017). Variability of the Pacific North Equatorial Current and its implications on Japanese eel (*Anguilla japonica*) larval migration. *Fish. Oceanogr.,* 26(3), 251-267. doi:10.1111/fog.12189

Ishikawa, S., Suzuki, K., Inagaki, T., Watanabe, S., Kimura, Y., Okamura, A., Otake, T., Mochioka, N., Suzuki, Y., Hasumoto, H., Oya, M., Miller, M.J., Lee, T-W., Fricke, H., and Tsukamoto, K. (2001). Spawning time and place of the Japanese eel *Anguilla japonica* in the North Equatorial Current of the western North Pacific Ocean. *Fish. Sci.,* 67, 1097–1103.

Jacoby, D. and Gollock, M. (2014). *Anguilla Japonica*. The IUCN Red List of Threatened Species 2014: e.T166184A1117791.

Kasai, A., Kishi, MJ., and Sugimoto, T. (1992). Modeling the transport and survival of Japanese sardine larvae in and around the Kuroshio Current. *Fish. Oceanogr.,* 1, 1-10.

Kasai, A., Komatsu, K., Sassa, C., and Konishi, Y. (2008). Transport and survival processes of eggs and larvae of jack mackerel *Trachurus japonicus* in the East China Sea. *Fish. Sci.,* 74, 8-18. doi: 10.1111/j.1444-2906.2007.01491.x

Kasai A., Yamazaki A., Ahn H., Yamanaka H., Kameyama, Masuda R., Azuma N., Kimura S., Karaki T., Kurokawa Y., and Yamashita Y. (2021). Distribution of Japanese eel *Anguilla japonica* revealed by environmental DNA, *Front. Ecol. Evol*., 9, 83. doi: 10.3389/fevo.2021.621461

Kida, S., Qiu, B., Yang, J., and Lin, X. (2016). The annual cycle of the Japan Sea Throughflow. *J. Phys. Oceanogr.,* 46, 23-39. doi: 10.1175/JPO-D-15-0075.1

Kim H, Kimura S, Shinoda A, Kitagawa T, Sasai Y, and Sasaki H. (2007) Effect of El Nino on migration and larval transport of the Japanese eel (*Anguilla japonica*). *ICES J. Mar. Sci.,* 64, 1387–1395. doi: 10.1093/icesjms/fsm091

Kimura, S., Tsukamoto, K., and Sugimoto, T. (1994). A model for the larval migration of the Japanese eel: roles of the trade winds and salinity front. *Mar. Biol.,* 119, 185–190. doi: 10.1007/BF00349555

Kimura, S., Inoue, T., and Sugimoto, T. (2001). Fluctuation in the distribution of low salinity water in the north equatorial current and its effect on the larval transport of the Japanese eel. *Fish. Oceanogr.,* 10, 51–60. doi: 10.1046/j.1365- 2419.2001.00159.x

Kimura, S. and Tsukamoto, K. (2006). The salinity front in the north equatorial current: a landmark for the spawning migration of the Japanese eel (*Anguilla japonica*) related to the stock recruitment. *Deep Sea Res. Part II: Topical Studies in Oceanography*, 53, 315–325. doi: 10.1016/j.dsr2.2006.01.009

Kumai, Y. and Kuroki, M. (2021). Salinity, freshwater and agricultural water preferences of glass eels of the Japanese eel *Anguilla japonica* collected in southern Japan. *J. Fish Biol.,* 99, 288-292. doi: 10.1111/jfb.14715

Kishida, T. and Kanto, I. (2013). Reconsideration on the catch of glass eel in Japan. *Bull. Jpn. Soc. Fish. Oceanogr.,* 77, 164-166. (in Japanese with English abstract)

Kanto, I. (2015). Indirect estimation about the amount of farmed production of Japanese eels *Anguilla japonica* in China by Using Alternative Data. *Bull. Jpn. Soc. Fish. Oceanogr*., 79, 61-66. (in Japanese with English abstract)

Kurogi, H., Okazaki, M., Mochioka, N., Jinbo, T., Hashimoto, H., Takahashi, M., Tawa, A., Aoyama, J., Shinoda, A., Tsukamoto, K., Tanaka, H., Gen, K., Kazeto, Y., and Chow, S. (2011) First capture of post-spawning female of the Japanese eel *Anguilla japonica* at the southern West Mariana Ridge. *Fish. Sci.,* 77, 199–205. doi: 10.1007/s12562-010-0318-3

Lalli, C. and Parsons, T., *Biological oceanography: an introduction*. Elsevier, 1997.

Lévy, M., Resplandy, L., Klein, P., Capet, X., Iovino, D., and Ethé, C. (2012). Grid degradation of submesoscale resolving ocean models: Benefits for offline passive tracer transport. *Ocean Modell.*, 48, 1-9. doi: 10.1016/j.ocemod.2012. 02.004

Lin, Y. F., Wu, C. R., and Han, Y. S. (2017). A combination mode of climate variability responsible for extremely poor recruitment of the Japanese eel (*Anguilla japonica*). *Sci. Rep.*, 7, 1-8. doi: 10.1038/srep44469

Liu, Z., Gan, J., Hu, J., Wu, H., Cai, Z., and Deng, Y. (2021). Progress on circulation dynamics in the East China Sea and southern Yellow Sea: Origination, pathways, and destinations of shelf currents. *Prog. Oceanogr.,* 193, 102553. doi: 10.1016/j.pocean.2021.102553

Otake, T., Inagaki, T., Hasumoto, H., Mochioka, N., and Tsukamoto, K. (1998). Diel vertical distribution of *Anguilla japonica* leptocephali. *Ichthyol. Res*., 45, 208–211. doi: 10.1007/BF02678565

Rypina, I. I., Llopiz, J. K., Pratt, L. J., and Lozier, M. S. (2014). Dispersal pathways of American eel larvae from the Sargasso Sea. *Limnol. Oceano.* 59, 1704-1714. doi: 10.4319/lo.2014.59.5.1704

Sakamoto, K., Tsujino, H., Nakano, H., Hirabara, M., and Yamanaka, G. (2013). A practical scheme to introduce explicit tidal forcing into an OGCM. *Ocean Sci.,* 9, 1089-1108. doi: 10.5194/os-9-1089-2013

Sakamoto, K., Tsujino, H., Nakano, H., Urakawa, S., Toyoda, T., Hirose, N., Usui, N., and Yamanaka, G. (2019). Development of a 2-km resolution ocean model covering the coastal seas around Japan for operational application. *Ocean Dyn.,* 69, 1181-1202. doi: 10.1007/s10236-019-01291-1

Shelton, A. O., Kelly, R. P., O'Donnell, J. L., Park, L., Schwenke, P., Greene, C., Henderson, R. A., and Beamer, E. M. (2019). Environmental DNA provides quantitative estimates of a threatened salmon species. *Biol. Conserv.*, 237, 383-391. doi: 10.1016/j.biocon.2019.07.003

Shinoda, A., Aoyama, J., Miller, M.J., Otake, T., Mochioka, N., Watanabe, S., Minegishi, Y., Kuroki, M., Yoshinaga, T., Yokouchi, K., Fukuda, N., Sudo, R., Hagihara, S., Zenimoto, K., Suzuki, Y., Oya, M., Inagaki, T., Kimura, S., Fukui, A., Lee, T. W., and Tsukamoto, K. (2011). Evaluation of the larval distribution and migration of the Japanese eel in the western north pacific. *Rev. Fish Biol. Fish.,* 21, 591–611. doi: 10.1007/s11160-010-9195-1

Tosi, L., Spampanato, A., Sola, C., and Tongiorgi, P. (1990). Relation of water odour, salinity and temperature to ascent of glass-eels, *Anguilla anguilla* (L.): a laboratory study. *J. Fish Biol.,* 36, 327-340. doi: 10.1111/j.1095-8649.1990.tb05613.x

Tsujino, H., Nakano, H., and Motoi, T. (2008). Mechanism of currents through the straits of the Japan Sea: Mean state and seasonal variation. *J. Oceanogr.,* 64, 141-161. doi: 10.1007/s10872-008-0011-7

Tsujino, H., Urakawa, S., Nakano, H., Small, R. J., Kim, W. M., Yeager, S. G., Danabasoglu, G., Suzuki, T., Bamber, J. L., Bentsen, M., Böning, C., Bozec, A., Chassignet, E. P., Curchitser, E., Dias, F. B., Durack, P. J., Griffiesn, S. M., Harada, Y., Ilicak, M., Josey, S. A., Kobayashi, C., Kobayashi, S., Komuro, Y., Large, W. G., Sommer J. L., Marsland, S. J., Masinas, S., Scheinert, M., Tomita, H.,

Valdivieso, M., and Yamazaki, D. (2018). JRA-55 based surface dataset for driving ocean-sea-ice models (JRA55-do). *Ocean Modell.,* 130, 79-139. doi:10.1016/j.ocemod.2018.07.002

Tsukamoto, K. (1992). Discovery of the spawning area for Japanese eel. *Nature,* 356, 789–791. doi: 10.1038/356789a0

Tsukamoto, K. (2006). Oceanic biology: spawning of eels near a seamount. *Nature,* 439, 929. doi: 10.1038/439929a

Tsukamoto, K. (2009.) Oceanic migration and spawning of anguillid eels. *J. Fish Biol*., 74, 1833–1852. doi: 10.1111/j.1095-8649.2009.02242.x.

Tsukamoto, K., Chow, S., Otake, T., Kurogi, H., Mochioka, N., Miller, M.J., Aoyama, J., Kimura, S., Watanabe, S., Yoshinaga, T., et al., (2011). Oceanic spawning ecology of freshwater eels in the western north Pacific. *Nat. Commun.,* 2, 179. doi: 10.1038/ncomms1174

Tzeng, W. N., Tseng, Y. H., Han, Y. S., Hsu, C. C., Chang, C. W., Di Lorenzo, E., and Hsieh, C. H. (2012). Evaluation of multi-scale climate effects on annual recruitment levels of the Japanese eel, *Anguilla japonica*, to Taiwan. *PLoS ONE*, 7, e30805. doi: 10.1371/journal.pone.0030805

Uchiyama, Y., Kuriyama, T. and Miyazawa, Y. (2012). Impact of the Kuroshio paths on oceanic and estuarine circulations in and around Seto Inland Sea. *J. JSCE*, Ser., B2 (Coastal Engineering), 68, I_441–I_445. (in Japanese with English abstract) doi: 10.2208/kaigan.68.I_441

Yamada, Y., Okamura, A., Mikawa, N., Utoh, T., Horie, N., Tanaka, S., Miller, M.J., and Tsukamoto, K. (2009). Ontogenetic changes in phototactic behavior during metamorphosis of artificially reared Japanese eel *Anguilla japonica* larvae. *Mar. Ecol. Prog. Ser*., 379, 241–251. doi: 10.3354/meps07912

Yoneta, A., Itakura, H., Arai, K., Kaifu, K., Yoshinaga, T., Miyake, Y., Shirai, K., and Kimura, S. (2019). Distribution of naturally recruited wild Japanese eels in Japan revealed by otolith stable isotopic ratios and document investigation. *Nippon Suisan Gakkaishi,* 85, 150–161. (in Japanese with English abstract) doi: 10.2331/suisan.18- 00038

Yoshinari, H., Higashi, H., and Nakada, S. (2020). Prediction of climate change impact of throughflow in the Seto Inland Sea using a land-ocean integrated model. *J. JSCE*, Ser., B2 (Coastal Engineering), 76(2), I_1105–I_1110. (in Japanese with English abstract) doi:10.2208/kaigan.76.2_I_1105

Zenimoto, K., Kitagawa, T., Miyazaki, S., Sasai, Y., Sasaki, H., and Kimura, S. (2009). The effects of seasonal and interannual variability of oceanic structure in the western Pacific North Equatorial Current on larval transport of the Japanese eel *Anguilla japonica*. *J. Fish Biol.,* 74, 1878-1890. doi.org/10.1111/j.1095-8649.2009.02295.x